INTERNATIONAL JOURNAL OF CIRCUITS, SYSTEMS AND SIGNAL PROCESSING
DOI: 10.46300/9106.2022.16.135 Volume 16, 2022

Leakage Detection and Localization of Water Pipeline Using Multi-features and Adaptive Time Delay Estimation

Yang Liu[1], Ze Chen[1], Zhongyan Liu[1], Xin Liu[1], Guochen Yu[1,*], Shun Na[1,2],
[1]College of Electronic Information Engineering, Inner Mongolia University, Hohhot, 010021, China
[2]College of Communication Engineering, Jilin University, Changchun, 130015, China

Received: May 8, 2022. Revised: June 16, 2022. Accepted: July 15, 2022. Published: September 16, 2022.

Abstract—The leakage of water in pipelines severely affects the environment and economy. However, there are limitations in the effectiveness of existing leak detection and localization techniques and methodologies. In this paper, we propose a novel leakage detection and localization method based on the multiple time-frequency features, a neural network, and an adaptive time delay estimation algorithm. First, we use spectral subtraction and wavelet denoising to reduce the effects of noise. In addition, to ensure and improve the accuracy of leakage detection in complex realistic environments, we propose the use of multi time-frequency features that can comprehensively represent the leak signal and make the neural network more robust to train a radial basis function (RBF)neural network to detect the leak signal. Further, we extract multiple features of the leakage signal and input into the RBF neural network to train. Moreover, to prevent the impulsive components of environmental noise and improve localization accuracy, we further propose the use of a fractional lower-order statistics (FLOS) based adaptive time delay estimation algorithm to estimate the time delay and locate the leakage. The simulation results show that the detection and localization performance of the proposed method is superior to those of existing schemes.

Keywords—leak detection and localization; spectral subtraction; wavelet; RBF; FLOS.

I. Introduction

Water is the most precious resource worldwide because it supports human activities, food production, and economic development [1]-[3]. However, a large amount of water is lost owing to leakages in underground water pipeline supply systems. Approximately 20% of the US water supply is lost through leaking pipes, and the corresponding amount in Europe is 16.5%–24.6%. Water loss caused by leakage results not only in a waste of natural resources but also causes a serious economic losses and public safety threats to all countries globally [4]-[6]. Therefore, it is necessary to detect these leakages as soon as possible and locate leakage points to prevent further damage to pipeline infrastructure and minimize water loss [7], [8].

Underground water pipeline systems are complicated, and leakage signals are affected by environmental and anthropogenic noise. In order, Various detection methods have been studied to detect the leakage in a timely and accurate manner. Traditional leakage detection techniques require extensive human involvement owing to visual inspection by personnel, therefore, they are time-consuming, labor-intensive, and have low reliability. In addition, these traditional leak detection techniques require labor-intensive human involvement and have poor leak detection reliability. Acoustic wave methods have received considerable attention for their fast-monitoring speed and high location accuracy [9]. These methods mainly use acoustic signal detectors and acoustic rods to listen to and measure sound waves. However, when the leakage point is deep in the ground or the background noise is large, the leakage signal weakens due to the absorption by the medium, thus, the performance of these methods with respect to the localization of the leakage point is poor [10], [11]. Many common leakage detection methods use sound and vibration sensors attached to the surface of the pipe to detect leaks, and locate them by using time delay estimation based on the correlation between the received signals of the two sensors [12], [13]. In recent years, some new neural networks based methods have been employed with the development of machine learning. [14] explored the use of deep learning for leak localization in water distribution networks (WDNs) using pressure measurements. In [15], a probabilistic decision support system based on artificial neural networks (ANNs) was proposed to detect the presence of leaks in pipeline transportation systems. In [16], a new hybrid of neural-adaptive tabu search (NATS) was proposed for leakage detection in pipelines. The proposed cooperative algorithms are formed from ANNs and adaptive tabu search (ATS). [17] proposed a water leakage detection system with an adaptive design that fuses a one-dimensional (1D) convolutional neural network and a support vector

machine to improve accuracy. In [18], a leakage detection and location method for the Tsumeb East area was presented using a support vector machine (SVM) and radial basis function (RBF) kernel. [19] reported the design of an in-pipe detector using neural networks to detect leak positions by analyzing the characteristics of leak signals. Compared with the traditional acoustic method, this method has a higher detection accuracy, however, the time domain signal is unstable and susceptible to noise interference.

When a leakage is detected from the pipeline, it is necessary to locate the leak positions rapidly and precisely. The existing cross-correlation based localization algorithms have the disadvantages of a lack of prior knowledge and statistical characteristics of the signal [20]. It is difficult to employ these methods in practical environments, since their detection performance is vulnerable to environmental and system noises. Although the time-frequency analysis technique that uses the short-time Fourier transform (STFT) can identify the leakage location in the case of very large environmental noise, it has limitations in terms of the analysis of sudden and nonstationary signals and cannot sensitively reflect the mutation. In [21], the authors proposed a method for leak location in water distribution systems based on low-frequency acoustic wave propagation, which locates leak positions by statistically processing the time delays associated with multiple acoustic paths in a noisy environment. [22] proposed a leak location technique for industrial fluid pipelines based on acoustic emission burst monitoring, which outperformed conventional generalized cross-correlation algorithms. However, in a complex environment, the acoustic emission signal may be distorted and easily interfered by environmental noise, resulting in a specific deviation in location, making the results less than ideal. Therefore, [23] proposed a new leak location method that combines cross-correlation with the time-spectrum segmentation of the acoustic signal, which can effectively identify the leak positions in the pipeline with a low error probability. Considering that underwater acoustic signals and environmental noise have different statistical characteristics, the least mean square (LMS) adaptive delay estimation algorithm provides leakage detection system with good tracking and adaptive capabilities [24]. In [25], an LMS adaptive time delay estimation algorithm was used for underground pipeline leakage location. To reduce the computational complexity and positioning error, a variable step-size signed adaptive filtering algorithm was introduced. In [26], bias-free LMS time delay estimation (LMSTDE) and real-time evaluation of the adaptive estimation result was proposed for water pipe leak detection and location by dynamically discriminating the convergence of adaption. However, these algorithms are based on the Gaussian distribution assumption, which is widely used because it supports for the central limit theorem (CLT). However, this assumption may limit the actual system recognition performance, such as in non-Gaussian impulse noise systems. Several physical experiments have confirmed that impulse noise frequently occurs in many systems, such as anthropogenic low-frequency atmospheric noise systems and water pipeline systems. Using an error criterion based on second-order statistics (SOS), the sparse-aware LMS algorithm may lead to poor performance or instability problems in such cases, particularly in the presence of strong impulse noise [27]. To address this problem, improved adaptive filtering algorithms have been developed. In [28], a novel error criterion was proposed for adaptive filtering, namely the smoothed least mean p-power (SLMP) error criterion, which aims to minimize the mean p-power of the error plus an independent and scaled smoothing variable. [29] proposed the derivation of the diffusion approximated kernel LMP (KLMP) algorithm by using random Fourier features to enhance the convergence performance. Nevertheless, limited research has been conducted on the background of underground water supply pipe leaks. Therefore, further investigations are required to obtain accurate and robust location algorithms.

In order to improve the accuracy and robustness of detection and positioning under the influence of environment, we propose a leakage detection and localization method for water pipelines based on multiple features, a neural network, and a fractional lower-order adaptive time delay estimation algorithm. The proposed method uses spectral subtraction and wavelet techniques to reduce the noise resulting from the pipeline leakage signals and enhance leakage signals. To improve the reliability and robustness of leakage detection, we use an RBF neural network trained by multiple features, including short-term energy, short-term zero-crossing rate, and spectral variance to detect the leakage. The proposed RBF neural network can effectively prevent noise and interference and overcome the limitations of traditional leakage detection methods based on a single time-frequency feature. Furthermore, to accurately locate the leakage point, we develop a leakage location approach based on the fractional lower-order statistics (FLOS) adaptive time delay algorithm, which does not require prior knowledge, is robust to both Gaussian and non-Gaussian impulsive noises, and improves the localization accuracy. The simulation results demonstrate that, compared with the existing schemes, our method can detect and localize the leakage point of a water pipeline more effectively.

The remain of this paper is organized as follows. Section 2 introduces the principles of leakage detection and location. In Section 3, we use spectral subtraction and wavelet transform to reduce noise and combine the multi-features of the leakage signal with the RBF neural network to improve the leakage detection accuracy. Then, we propose an FLOS-based adaptive time delay estimation method for leakage location. Our simulation results are provided in Section 4 to verify the advantages of the proposed scheme. Finally, the conclusions are presented in Section 5.

II. Preliminary

The leakage detection and location model are shown in Fig. 1, where the sensors are distributed on the water supply pipeline, L is the distance between two sensors located at the

two sides of the pipeline leakage, and d_1 and d_2 are the distances from the leakage point to nodes 1 and 2, respectively We define $L = d_1 + d_2$.

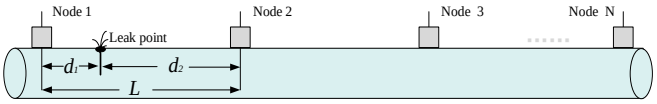

Figure 1. Schematic diagram of leakage point location

When a leakage occurs, an acoustic vibration signal is generated at the leakage point, spreads in two directions and can be received by the sensors on both sides. The leakage signals received by the sensors have similar waveforms and different time delays and noises, which can be represented as follows:

$$x_i(t) = s(t - t_i) + n_i(t),\ i = 1, 2, ..., \quad (1)$$

where $s(t)$ is the leakage signal, t_i is the time delay between the leak point and sensor i, and $n_i(t)$ is the received noise of sensor i. The time delay between sensor i and sensor j can be expressed as

$$\tau_{ij} = t_i - t_j = \frac{d_i - d_j}{v}, \quad (2)$$

where v denotes the transmission velocity of the leakage signals in the pipeline. When the distance between the leak point and sensors is known, the velocity v can be estimated. In general, the distance between the two sensors and the signal transmission velocity v are known or can be obtained from the measurements. As a result, equation (1) and (2) can be used to calculate the distances from a leakage to each of the two sensors, e.g., when i, j=1, 2,

$$\begin{cases} d_1 = \dfrac{L - \tau v}{2} \\ d_2 = \dfrac{L + \tau v}{2} \end{cases} \quad (3)$$

Therefore, it is sufficient to detect the leakage position by receiving $x_i(t)$ and estimating the time delay of the leakage signals received by at least two different sensors. The estimated delay value is used to calculate the distance between the leak point and a sensor to locate the leak point.

III. Proposed Leakage Detection and Location Method

A. Noise reduction method

In the detection and positioning of water leakage, due to the significant influence of various noises in the environment, leakage sound signals superimposed with noise signals affect the detection and positioning accuracy of the leakage location. To improve detection and positioning accuracy, it is importance to denoise the leakage signal in advance. Spectral subtraction is the most commonly used sound enhancement technology, and is characterized by a small number of calculations and ease of implementation. The basic idea is to assume that the noise is stationary or changes slowly short-time stationary additive noise, and that the desired signal and noise are independent of each other. This method removes the noise from the original signal, and a pure signal can be obtained.

In this paper, the object of spectral subtraction processing is the acoustic signal leakage in water leakage detection. The Fourier transform of one frame can be written as follows:

$$X_i(k) = \sum_{m=0}^{N-1} x_i(m) \exp(-j \frac{2\pi nk}{N}), k = 0, 1, ..., N-1, \quad (4)$$

where $x_i(m)$ is the i th frame of the original leakage signal after windowing and frame processing, and N is the length of the signal frame. The magnitude of $X_i(k)$ is $|X_i(k)|$, and the phase of $X_i(k)$ is given by the following equations

$$X_{angle}^{i}(k) = \arctan\left[\frac{\mathrm{Im}(X_i(k))}{\mathrm{Re}(X_i(k)}\right]. \quad (5)$$

The average power of the noise is expressed as

$$D(k) = \frac{1}{M} \sum_{i=1}^{M} |D_i(k)|^2, \quad (6)$$

where $D_i(k)$ is the Fourier transform of the noise $n_i(m)$. The power spectrum of the leakage signal with noise reduction can then be obtained by subtracting the noise power spectrum from the power spectrum of the original leakage signal. Using the spectral subtraction, we can obtain the power spectrum of the leakage signal,

$$\left|\hat{X}_i(k)\right|^2 = \begin{cases} |X_i(k)|^2 - a \cdot D(k), \left|\hat{X}_i(k)\right|^2 \geq a \cdot D(k) \\ b \cdot D(k), \left|\hat{X}_i(k)\right|^2 \leq a \cdot D(k) \end{cases}, \quad (7)$$

where a is the attenuation factor, and b is the gain compensation factor.

To further reduce the influence of noise, wavelet decomposition is used to remove the noise. The wavelet threshold denoising method is the most widely used method in practical engineering [30], [31]. In practical applications, leakage signals usually appear as specific low-frequency signals or relatively stable signals, whereas noise contain more high-frequency and impulsive components. Therefore, we perform three-layer decomposition wavelet decomposition on the received signal as,

$$x = cA_1 + cD_1 = cA_2 + cD_2 + cD_1 = cA_3 + cD_3 + cD_2 + cD_1, \quad (8)$$

where x is the leakage signal after the spectral subtraction process, and cA_i and cD_i are the approximate parts and details of x, respectively. Noise is usually included in cD_i.

In general, the coefficients of the signal are larger than the coefficients of noise after wavelet decomposition, so we can find a suitable value for λ as the threshold. In this paper, we use the soft threshold method to reconstruct the denoised signal using the obtained wavelet coefficients. The soft threshold function is given by

$$\bar{w}_{ij} = \begin{cases} sgn(W_{j,k})(|W_{j,k}| - \lambda), |W_{j,k}| \geq \lambda \\ 0, |W_{j,k}| \leq \lambda \end{cases}, \quad (9)$$

where $W_{j,k}$ and $\overline{w}_{ij}$ are wavelet coefficients before and after denoising, respectively, and $sign(\cdot)$ is the sign function. Therefore, we need to choose a suitable method for calculating the threshold λ. The most important part of wavelet denoising is selecting the threshold function and estimating the threshold. The principle of threshold selection based on sample estimation is to estimate the signal, determine a unified threshold value, retain the coefficients that are larger than the threshold value, and intercept the coefficients that are smaller than the threshold value. To preserve the signal integrity, we develop an adaptive threshold selection method based on Stein's unbiased likelihood estimation (Rigrsure). We take the absolute value of each element of the signal $x(m)$ and sort them in increasing order. Subsequently, each element is squared to obtain a new sequence [32],

$$\hat{x}(k) = (sort(|x|))^2, k = 0,1,...,N-1, \quad (10)$$

where $sort(|x|)$ refers to the sorting $|x|$ from small to large. It is assumed that the threshold is the square root of the *k*-th element of $\hat{x}(k)$, which is defined as $\lambda = \sqrt{\hat{x}(k)}$. The risk generated by this threshold is expressed as

$$Rish(k) = \left[N - 2k + \sum_{i=1}^{k} \hat{x}(i) + (N-k)\hat{x}(N-k) \right] \Big/ N. \quad (11)$$

According to the risk function $Rish(k)$, the value corresponding to the minimum risk point of the curve is denoted by $k_{\min}$, and the rigrsure threshold can then be defined as $\lambda = \sqrt{\hat{x}(k_{\min})}$. After denoising the water leakage signal with a wavelet, the noise suppression is apparent and the leakage signal is enhanced.

B. Leakage detection based on multi-features and RBF neural network

In this paper, to detect the leakage signals, we use an RBF neural network, which is a multilayer feedforward neural network. The mapping relationship is determined when the center point of the RBF neural network is determined; the mapping from the hidden layer space to the output space is linear. In other words, the output of the network is the linear weighted sum of the outputs of the hidden units. The weight is a network adjustable parameter. In general, the mapping of the network from the input to the output is nonlinear, whereas the network output is linear for adjustable parameters. Thus, the weights of the network can be solved directly by system of linear equations. Consequently, the learning speed is significantly accelerated and local minimum problems are prevented.

The structure of the RBF neural network is similar to that of other feedforward neural networks. It comprises three layers: the input, hidden, and output layer, as illustrated in Fig. 2. The nodes within each layer were fully connected to the previous layer, and the input nodes are directly connected to the hidden layer neurons.

As shown in Fig.2, the first layer is the input layer, which consists of leakage signal source nodes and transmits input information to the hidden layers. In the hidden layer, the input variables are mapped to their space, which is a nonlinear transformation. Note that the use of a larger number of neuron nodes in the hidden layer enables the better mapping capabilities. Nevertheless, a superior mapping ability requires

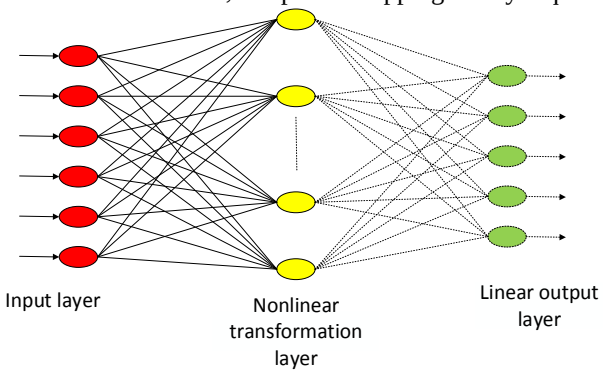

Figure 2. Topology of RBF neural network

higher network complexity. Finally, the output layer produces weighting data with a linear process, and this output is used as the direct target of the model output of the RBF networks in training [33]. The mathematical model of an RBF neural network with N hidden layer neurons can be expressed as:

$$y = \sum_{n=1}^{N} w_n a_n(\mathbf{x}), \quad (12)$$

where $\mathbf{x} = (x_1, x_2, ..., x_M)^T$ is the input vector, y is the output vector of the network, M is the number of input variables, w_n is the weighting coefficient connecting the hidden neuron and output layer, and $a_n(\mathbf{x})$ is the output value of the *n*-th hidden layer neuron node,

$$a_n(\mathbf{x}) = \exp\left(-\|\mathbf{x} - \mathbf{c}_n\| / 2\sigma_n^2\right), n = 1,2,...N, \quad (13)$$

where $\mathbf{c}_n$ is the center vector of the *n*-th hidden neuron, $\|\mathbf{x} - \mathbf{c}_n\|$ is the Euclidean distance between $\mathbf{x}$ and $\mathbf{c}_n$, and σ_n is the radius or width of the *n*-th hidden neuron. Equation (13) is the Gaussian function, which is commonly used in RBF. We choose a Gaussian function because its representation is simple and does not require much complexity, even for multivariable inputs. In addition, it has good analytical properties and is convenient for theoretical analyses. To construct and train an RBF neural network, the center c_i, variance σ_n, and weight w_i of each basis function are determined by the mapping function through learning. Finally, the input-output is completed. The realization of a nonlinear transformation from the input layer to the hidden layer of the RBF network depends on the number, location, and scope width of the RBF centers. As the random selection center method requires a large training set to achieve a satisfactory performance, we adopt the self-organizing learning method. The center of the RBF can be moved, and its position is determined by self-organizing learning, whereas the linear weight of the output layer is calculated by supervised learning.

First, we use the K-means clustering method to determine the

width of the neuron center and Gaussian function.

1) From the input samples $x_n(n=1,2,...,N)$, we select N_r samples randomly as the initial cluster centers $c_i(1 \le i \le N)$ (the final number of centers is also N_r).
2) The input samples are grouped according to the nearest-neighbor principle. At a certain time t, the Euclidean distance between each new input vector $x_n(t)$ and each cluster center is calculated, and the minimum distance is obtained by
$$a_i(t) = \|x_n(t) - c_i(t)\|, 1 \le i \le N_r, \quad (14)$$
$$k = \arg[\min\{a_i(t), 1 \le i \le N_r\}]. \quad (15)$$
3) After assigning the sample to the nearest center, the cluster center is recalculated as
$$c_k(t+1) = \begin{cases} c_k(t) + \eta[x_n(t) - c_k(n)], k = k(x_n) \\ c_k(t), \text{others} \end{cases}, \quad (16)$$
where $\eta(0 < \eta < 1)$ is the learning rate.
4) After classifying all the samples, we compare the new cluster center with the previous cluster center and determine whether there is any change in the classification. If so, continue Steps (2) and (3) are continued, otherwise the calculation is stopped.

We can determine the center of the hidden layer neurons according to the above steps, and the variance of the RBF can then be calculated by
$$\sigma_i = d_m / \sqrt{2N_r} \quad (17)$$
where d_m is the maximum distance between the selected centers. The weights w between the hidden layer and the output layer are derived using the least squares algorithm in the supervised learning phase.
$$w = \exp(\frac{N_r}{d^2_m} \|X_n - c_i\|^2) \quad (18)$$

To ensure and improve the accuracy of leakage detection in a complex realistic environment, we propose to use multi time-frequency features as the input to train the RBF neural network. The features can comprehensively represent the leak signal and render the neural network more robust for detecting the leakage signals. The multi-features include short-time energy $E(i)$, short-time average zero-crossing rate $Z(i)$, and spectrum variance $D(i)$ [34], [35]. We assume that the original acoustic signal is $x(n)$, and after the frame processing, we can get $y_i(n)$, $1 \le i \le F$, where F is the total number of frames. These features can be expressed as
$$E(i) = \sum_{n=0}^{N-1} y_i^2(n), 1 \le i \le F, \quad (19)$$
$$Z(i) = \frac{1}{2} \sum_{n=0}^{N-1} |\text{sgn}[y_i(n)] - \text{sgn}[y_i(n-1)]|, 1 \le i \le F. \quad (20)$$
The spectrum $X_i(k)$ of the frame signal $y_i(n)$ is obtained by a discrete Fourier transform, and the spectrum variance is denoted as
$$D_i = \frac{1}{N} \sum_{k=0}^{N-1} \left[|X_i(k) - E_i| \right]^2, 1 \le i \le F, \quad (21)$$
where N is the frame length. $\text{sgn}(\cdot)$ is the sign function, and E_i is the mean of $X_i(k)$, which is defined as
$$E_i = \frac{1}{N} \sum_{k=0}^{N-1} |X_i(k)|. \quad (22)$$

The short time energy is the energy of the short acoustic segment, which can classify the useful and useless components of an acoustic signal simply and effectively. The short-time average zero-crossing rate reflects the frequency distribution of the signal, the high frequency part has a high zero crossing rate, while the low frequency part has a low zero crossing rate. The spectrum variance reflects the degree of fluctuation degree in the energy change of frequency domain. For a white noise signal where no leakage occurs, its energy is small and the fluctuation is relatively gentle, thus, the spectrum variance is small. When a leak occurs, the variance of the spectrum of the leak signal increases, and we can determine the endpoint of the leak signal based on the variance of the spectrum. Subsequently, we input the training samples into the trained neural network and compared the obtained output with the marked leakage signal segment. If the result is the same as the marked result, the established RBF neural network model can effectively monitor the leakage signal. If the accuracy of the test result is low, the training of the neural network is considered insufficient, and it needs to be retrained. Repeat This step is repeated until requirements are met.

C. Location of leakage point using FLOS-based adaptive time delay estimation

The leakage signal is transmitted through a pipeline, and can be received by different sensors. The signals received by the two sensors can be represented as
$$\begin{cases} x_1(n) = s(n) + n_1(n) \\ x_2(n) = as(n-D) + n_2(n) \end{cases}, \quad (23)$$
where $s(k)$ is the leakage source signal from the leakage point, a represents the attenuation factor between the sensors 1 and 2, D is the relative time delay of the leakage signal between these two sensors, and $n_1(k)$ and $n_2(k)$ are the received noises.

We use an adaptive filter to estimate the relative time delay of the two received signals, and the leak point is located through the time delay using equation (3). A received signal x_1 serves as the input signal x_k of the adaptive filter, and the other observation signal x_2 serves as the desired signal d_k. Since the time delay can be positive or negative, the order of the filter is set to $2N+1$, where N is the maximum order of the filter in the positive or negative direction. In actual applications, leakage signals are affected by numerous factors, including pipe material, pipe diameter, pressure in the pipe, flow rate, leakage status, etc. In addition, the environmental noise that overlaps with the leakage signals can be extremely severe. In particular, because most water pipelines are laid in heavily populated urban areas, numerous studies have indicated that urban

environmental noise, including traffic noise and mechanical construction noise, is non-Gaussian impulse noise with significant pulse characteristics. In non-Gaussian noise models, the minimum mean square error criterion cannot be used because the signal or noise has no second-order statistics such as variance. However, the fractional low-order statistics of the signal or noise can be calculated. In this case, instead of the original variance, the dispersion coefficient can be used. The average amplitude is minimized when the dispersion coefficient is minimized. Several studies have shown that minimizing the dispersion coefficient is equivalent to minimizing the probability of estimation errors. Therefore, we make better use of FLOS based adaptive filters to solve the complex conditions of the leak detection environment and enhance the robustness of the delay estimation.

Considering the severe noise, stability, and convergence speed of the algorithms, the system uses the normalized least mean p th-power (NLMP) algorithm. In general, for a random variable, its second-order moment is defined as $E[x(n)^2]$. For a non-Gaussian α stable distribution random variable, its fractional low-order moment is defined as $E[|x(n)|^p]$, where $0 \le p < \alpha \le 2$. The weight vector $\mathbf{w}(n)$ is updated by the stochastic gradient as

$$\mathbf{w}(n+1) = \mathbf{w}(n) - \mu \mathbf{x}(n) \frac{|e(n)|^{p-1} \operatorname{sgn}(e(n))}{\|\mathbf{x}(n)\|_p^p + \varsigma}, \quad (24)$$

where μ is the step size length, ς is the normalization coefficient $(\varsigma > 0)$, $\|\cdot\|_p$ is the p -norm of the signal, and $p < \alpha$ (α is the characteristic exponent of the signal). The error signal is $e(n) = d(n) - x(n)$, and the estimated time delay is the coordinate corresponding to the largest weight vector,

$$\hat{D} = \arg\max_k [w_{opt}], k = -N, -N+1, ..., N. \quad (25)$$

Therefore, the distances between the leakage point and nodes 1 and can be obtained by $\hat{L}_1 = \frac{L + v\hat{D}}{2}$ and $\hat{L}_2 = \frac{L - -v\hat{D}}{2}$, respectively, so we can obtain the exact location of the leakage point.

One advantage of the NLMP algorithm is that it has broad applicability depending on the setting of the parameter p. In equation (25), if $p = 2$, the NLMP algorithm becomes the LMS and normalized LMS (NLMS). If $p = 1$, the NLMP algorithm becomes the normalized least mean absolute deviation (NLMAD). In actual applications, p should be selected based on the characteristic exponent of the signal α $(0 < \alpha \le 2)$ to ensure that the algorithm performs well.

Accordingly, the characteristic exponent α must be estimated before applying this algorithm. For X_k $(k = 1, 2, ..., N)$, we define $Y_k = \log|X_k|$, and the variance of Y can be expressed as,

$$\operatorname{Var}(Y) = \frac{\pi^2}{6}\left(\frac{1}{\alpha^2} + \frac{1}{2}\right). \quad (26)$$

Using the signal sample, the variance in can be estimated as

$$\hat{\sigma}_Y^2 = \frac{\sum_{i=1}^{N} (Y_i - \bar{Y})^2}{N-1}, \quad (27)$$

where $\bar{Y} = \sum_{i=1}^{N} Y_i \Big/ N$ is the average value of Y for the sample. By using equations (26) and (27), we can obtain the estimates

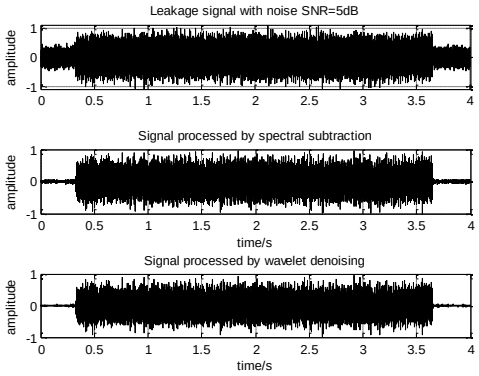

Figure 3a. The waveform of leakage signal processed by spectral subtraction and wavelet denoising (Leakage signal with SNR= 5 dB).

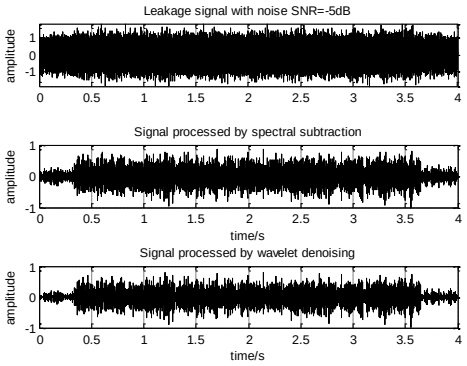

Figure 3b. The waveform of leakage signal processed by spectral subtraction and wavelet denoising (Leakage signal with SNR= -5 dB).

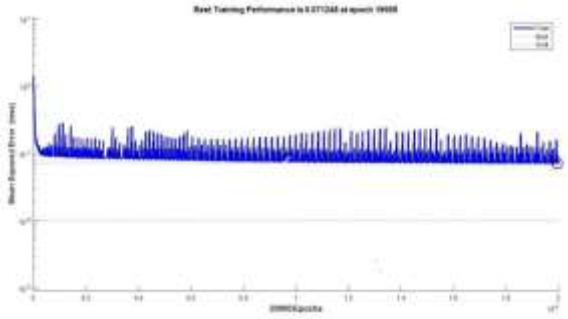

Figure 4. RBF neural network training curve of α.

IV. Simulation of the System

A. Simulation of leak detection

In this environment, we use sensors with a sampling rate of 1000 kbps. Fig. 3 shows the waveform of the water leakage signal after spectral subtraction and wavelet denoising processing. This demonstrates that the environmental noise is removed obviously after the leakage signal is successively processed by spectral subtraction and wavelet denoising. Table. 1 shows the denoising performance. The denoising effect is better at lower signal-to-noise ratio (SNR), which can be attributed to the reliability of the proposed leakage detection method.

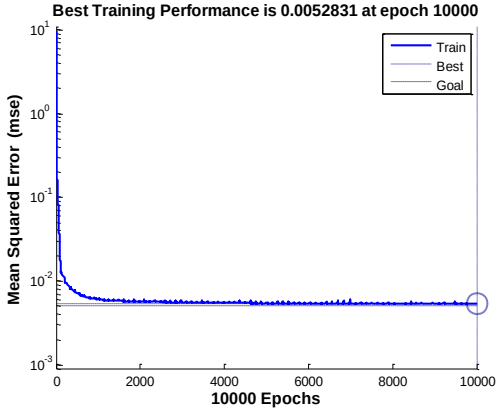

Figure 5a. Network training performance when SNR=10 dB

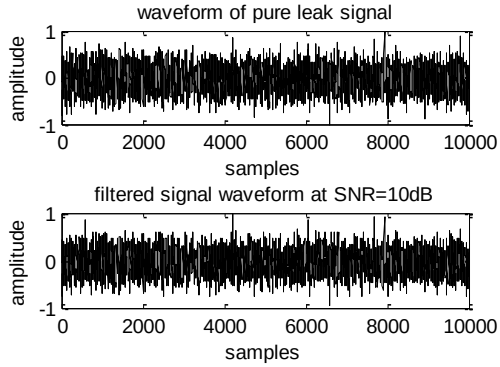

Figure 5b. The waveform of pure leak signal and filtered signal when SNR=10 dB

Table. 1. SNR enhancement results

Initial SNR (dB)	5	3	1	0	-1	-2	-3	-4
SNR after denoising(dB)	6.2	4.8	3.4	2.8	2.3	1.8	1.4	1

To improve the accuracy of the leakage detection method, multiple features of the leakage signal are extracted and input into the RBF neural network. First, the RBF neural network is modeled. The short-time energy, short-time zero-crossing rate, and spectrum variance of the leakage signal are inputted into the modeled RBF neural networks. After 2000 experiments, we use 20 nodes in the hidden layer. The results are shown in Fig. 4. After 20,000 training sessions, the best training effect is achieved in the 19959th epoch, and the mean square error is reduced to 0.0712.

Fig. 5 and Fig. 6 show the neural network training performance at different SNR. The SNR is set in the range of 10 to -8 dB to allow the signal to pass through the neural network, and the number of hidden layer nodes is set to 20 and 10000 epochs. Fig. 5(b) and Fig. 6(b) show that although the filtering effect of the neural network becomes worsens when the SNR is -4 dB, the proposed neural network can still converge. It should be noted that the parameter settings of the network itself also affect the positioning accuracy, and the parameters of the RBF neural network mainly include the number of nodes in the hidden layer, transmission function, and training method. The

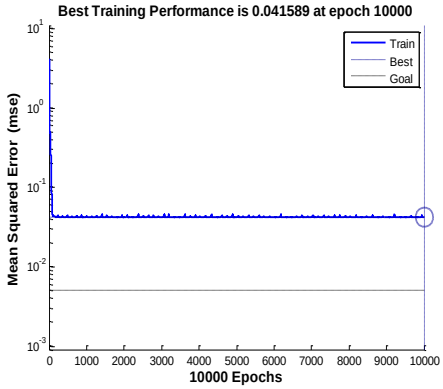

Figure 6a. Network training performance when SNR= -4 dB

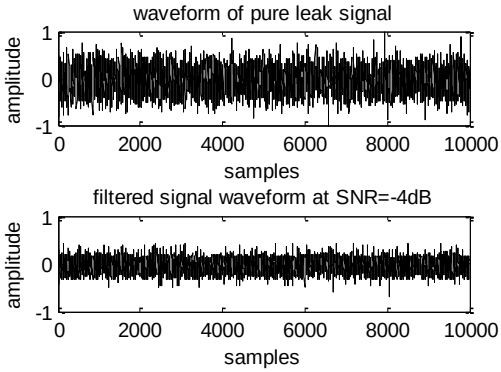

Figure 6b. The waveform of pure leak signal and filtered signal when SNR= -4 dB

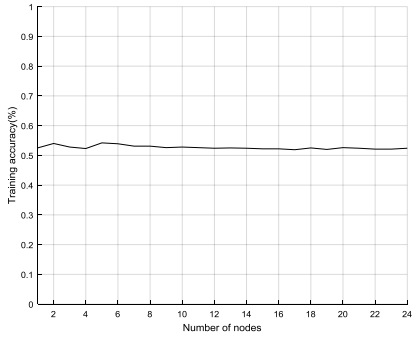

Figure 7. Neural network training accuracy of different hidden layer nodes

experimental object is set as a water leakage signal containing Gaussian white noise with SNR of 10 dB, which is trained in the network containing different numbers of nodes of the hidden layer, changing the number of nodes of the hidden layer, and conducting several training sessions to obtain the mean value of the training accuracy. As shown in Fig. 7, the optimal number of nodes of the hidden layer is 17, and the training error accuracy is the smallest at 0.00519. The results indicate that the number of nodes has little effect on the training accuracy, but training accuracy stabilizes as the number of nodes increases.

B. Simulation of leak location

To test the performance of the time delay estimation algorithm, as the original signals, we employed signals that had been sampled by two sensors on both sides of a leakage point located 18 m from the leakage point during quiet periods of

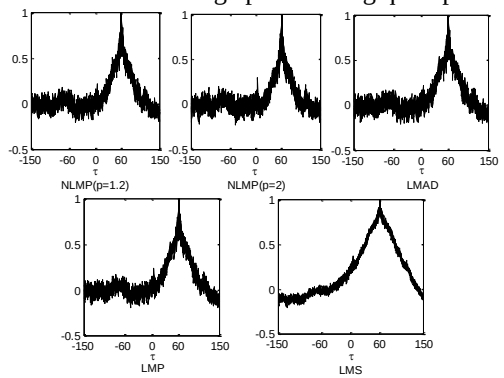

Figure 8a. Time delay estimation results obtained using several types of self-adaptive algorithms: Gaussian noise

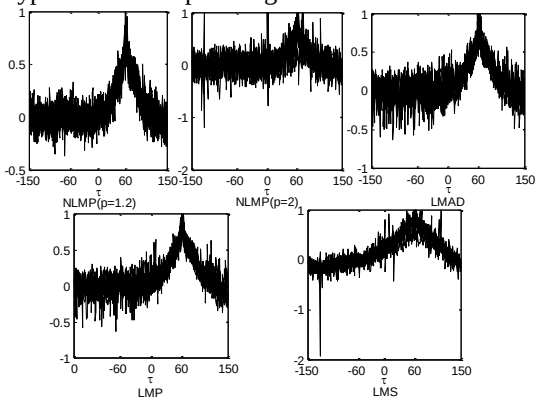

Figure 8b. Time delay estimation results obtained using several types of self-adaptive algorithms: Impulse noise

time as the original signals. The system has a sampling frequency of 5 kHz, and acoustic signals are transmitted through the pipeline at a velocity of approximately 1500 m/s. Thus, the two sensors have a time delay of 60 samples. Based on equations (26) and (27), the characteristic exponent of the signals are estimated as $\hat{\alpha}_1$=1.8696 and $\hat{\alpha}_2$=1.8759. These results indicate that leakage signals have relatively weak impulsive characteristics, even during quiet periods.

Fig. 8 shows the time delay estimation results obtained from 10 independent simulations in the presence of 0 dB Gaussian noise and impulse noise (α=1.7), respectively. Fig. 9 shows the convergence of algorithms under Gaussian noise and impulse noise. The fractional lower order coefficient p for the NLMP is 1.2 and 2, respectively, and for LMAD and the least mean p power (LMP) is 1.2. The results in Fig. 8 show that all of the algorithms exhibit a relatively good performance in Gaussian noise environment and can be used to precisely estimate the time delay values. However, in the impulsive noise environment, the performance of the NLMP (p=2) and LMS algorithms deteriorate significantly. This is because when p=2, NLMP becomes NLMS, and the second-order statistics based NLMS and LMS algorithms cannot overcome impulsive noise. In contrast, the NLMP (p=1.2), LMP, and LMAD algorithms can effectively overcome impulsive noise, and the NLMP algorithm (p=1.2) offers excellent time delay estimation performance. The results shown in Fig. 9 reveal that

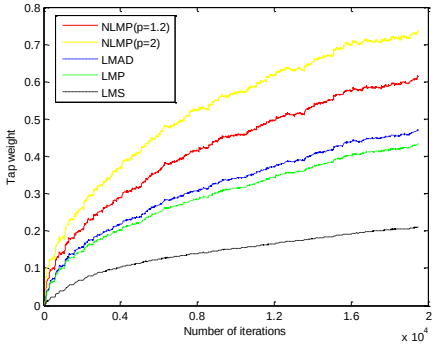

Figure 9a. Convergence performance of several types of self-adaptive algorithms: Gaussian noise

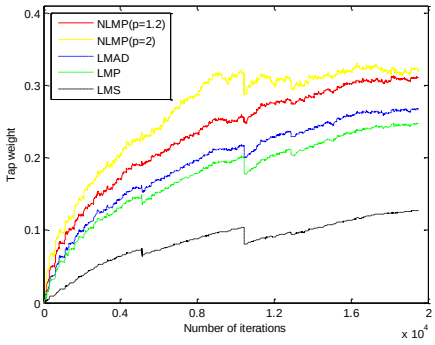

(b)

Figure 9b. Convergence performance of several types of self-adaptive algorithms: Impulse noise

when a reasonable fractional lower-order factor ($p<\alpha$) is selected, NLMP can effectively suppress the effects of Gaussian noise and impulsive noise and has excellent time delay estimation and convergence performance.

V. Conclusions

This paper proposes a leakage detection and location method based on multiple features, RBF neural network, and FLOS-based adaptive delay estimation. First, we use spectrum subtraction and wavelet denoising methods to reduce the background noise and improve the SNR of the leakage signal.

We then train an RBF neural network to detect water leakage signals using multi-time-frequency features as the input vectors. In addition, we propose an adaptive delay estimation method based on FLOS to estimate the time delay that can be used to locate the leakage point between sensors. The detection accuracy is good even in the case of a low SNR, and it can adapt to the complex underground water pipeline environment. Meanwhile, the proposed FLOS-based time-delay estimation algorithm can suppress the effects of Gaussian noise and impulse noise more effectively than the traditional estimation algorithm. Furthermore, it has good time-delay estimation and convergence performance, thus improving the accuracy of leak localization. Based on the simulation and experimental results of the Gaussian noise model and non-Gaussian noise model, it can be seen that the proposed method can effectively distinguish between the leakage signal and noise and accurately locate the leakage point.

VI. Acknowledgments

The authors are grateful to the National Science Foundation of China for its support of this research. This work was supported in part by the National Science Foundation of China under Grant 62161037 and162071257, and is supported in part by the Program for Young Talents of Science and Technology in Universities of Inner Mongolia Autonomous Region under Grant NJYT-20-A11, and in part by the Natural Science Foundation of Inner Mongolia Autonomous Region under Grants 2019MS06033.

References

[1] M. Kothandaraman, Z. Law, E. M. A. Gnanamuthu and C. H. Pua, "An Adaptive ICA-Based Cross-Correlation Techniques for Water Pipeline Leakage Localization Utilizing Acousto-Optic Sensors," in IEEE Sensors Journal, vol. 20, no. 17, pp. 10021-10031, 1 Sept.1, 2020.

[2] J. Harmouche and S. Narasimhan, "Long-Term Monitoring for Leaks in Water Distribution Networks Using Association Rules Mining," in IEEE Transactions on Industrial Informatics, vol. 16, no. 1, pp. 258-266, Jan. 2020.

[3] M. Zhou, Z. Pan, Y. Liu, Q. Zhang, Y. Cai and H. Pan, "Leak Detection and Location Based on ISLMD and CNN in a Pipeline," in IEEE Access, vol. 7, pp. 30457-30464, 2019.

[4] M. I. Mohd Ismail et al., "A Review of Vibration Detection Methods Using Accelerometer Sensors for Water Pipeline Leakage," in IEEE Access, vol. 7, pp. 51965-51981, 2019.

[5] A. Purwar, M. Patel, M. Garg and K. Ahuja, "A Novel Approach for Water Leakage Detection and Localization," 2018 7th International Conference on Reliability, Infocom Technologies and Optimization (Trends and Future Directions) (ICRITO), Noida, India, 2018, pp. 373-377.

[6] J. Li, C. Wang, Q. Zheng and Z. Qian, "Leakage Localization for Long Distance Pipeline Based on Compressive Sensing," in IEEE Sensors Journal, vol. 19, no. 16, pp. 6795-6801, 15 Aug.15, 2019.

[7] S. Li, C. Xia, Z. Cheng, W. Mao, Y. Liu and D. Habibi, "Leak Location Based on PDS-VMD of Leakage-Induced Vibration Signal Under Low SNR in Water-Supply Pipelines," in IEEE Access, vol. 8, pp. 68091-68102, 2020.

[8] J. Kang, Y. Park, J. Lee, S. Wang and D. Eom, "Novel Leakage Detection by Ensemble CNN-SVM and Graph-Based Localization in Water Distribution Systems," in IEEE Transactions on Industrial Electronics, vol. 65, no. 5, pp. 4279-4289, May 2018.

[9] Shuxin Yin,Yunfei Liu,Wei Han. Single-point location algorithm based on an acceleration sensor for pipeline leak detection[J]. Measurement,2020,163(prepublish).

[10] D. C. Ferino, R. P. Jose, J. R. M. Ochoa, V. V. Villamiel and J. Meynard P. Araña, "Development of Leak Detection System for PVC Pipeline Through Vibro-Acoustic Emission," TENCON 2018 - 2018 IEEE Region 10 Conference, Jeju, Korea (South), 2018, pp. 2557-2560.

[11] Z. Zhong, J. Suzuki, T. Miyake, H. Kondou and K. Enastu, "Study on water leak detection using wavelet instantaneous cross-correlation," 2015 International Conference on Wavelet Analysis and Pattern Recognition (ICWAPR), Guangzhou, 2015, pp. 133-137.

[12] P. Karkulali, H. Mishra, A. Ukil and J. Dauwels, "Leak detection in gas distribution pipelines using acoustic impact monitoring," IECON 2016 - 42nd Annual Conference of the IEEE Industrial Electronics Society, Florence, 2016, pp. 412-416.

[13] Choi, J.; Shin, J.; Song, C.; Han, S.; Park, D.I. "Leak Detection and Location of Water Pipes Using Vibration Sensors and Modified ML Prefilter". Sensors 2017, 17, 2104.

[14] M. Javadiha, J. Blesa, A. Soldevila and V. Puig, "Leak Localization in Water Distribution Networks using Deep Learning," 2019 6th International Conference on Control, Decision and Information Technologies (CoDIT), Paris, France, 2019, pp. 1426-1431.

[15] M. B. Abdulla, R. O. Herzallah and M. A. Hammad, "Pipeline leak detection using artificial neural network: Experimental study," 2013 5th International Conference on Modelling, Identification and Control (ICMIC), Cairo, 2013, pp. 328-332.

[16] S. Sornmuang, J. Suwatthikul and S. Thirachai, "Leak detection of pipeline using a hybrid of Neural-Adaptive Tabu Search algorithm," 2014 14th International Conference on Control, Automation and Systems (ICCAS 2014), Seoul, 2014, pp. 531-534.

[17] J. Kang, Y. Park, J. Lee, S. Wang and D. Eom, "Novel Leakage Detection by Ensemble CNN-SVM and Graph-Based Localization in Water Distribution Systems," in IEEE Transactions on Industrial Electronics, vol. 65, no. 5, pp. 4279-4289, May 2018.

[18] J. Kemba, K. Gideon and C. N. Nyirenda, "Leakage detection in Tsumeb east water distribution network using EPANET and support vector regression," 2017 IST-Africa Week Conference (IST-Africa), Windhoek, 2017, pp. 1-8.

[19] Wang, Wenming, et al. "Experimental study on water pipeline leak using In-Pipe acoustic signal analysis and

artificial neural network prediction." Measurement 186 (2021): 110094.

[20] K. B. Adedeji, Y. Hamam, B. T. Abe and A. M. Abu-Mahfouz, "Towards Achieving a Reliable Leakage Detection and Localization Algorithm for Application in Water Piping Networks: An Overview," in IEEE Access, vol. 5, pp. 20272-20285, 2017.

[21] Kafle, Marshal Deep, Stanley Fong, and Sriram Narasimhan. "Active acoustic leak detection and localization in a plastic pipe using time delay estimation." Applied Acoustics 187 (2022): 108482.

[22] Quy, Thang Bui, and Jong-Myon Kim. "Leak localization in industrial-fluid pipelines based on acoustic emission burst monitoring." Measurement 151 (2020): 107150.

[23] G. -P. Kousiopoulos, N. Karagiorgos, D. Kampelopoulos, V. Konstantakos and S. Nikolaidis, "Dealing with stochastic signals and physical phenomena impacting pipeline leak localization accuracy," 2021 IEEE International Instrumentation and Measurement Technology Conference (I2MTC), 2021, pp. 1-6, doi: 10.1109/I2MTC50364.2021.9459830.

[24] Yumei Wen, Ping Li, Jin Yang and Zhangmin Zhou, "Information processing in buried pipeline leak detection system," International Conference on Information Acquisition, 2004. Proceedings., Hefei, 2004, pp. 489-493.

[25] L. Zhonghu, G. Meili, L. Wentao and W. Luling, "Research of adaptive algorithm in water supply pipeline leak location," 2017 IEEE International Conference on Signal Processing, Communications and Computing (ICSPCC), Xiamen, 2017, pp. 1-5.

[26] H. Wu, Y. Wen, J. Yang and P. Li, "Adaptive detection and location for water pipeline leaks in lower SNR and nonstationary environments," 2009 IEEE International Conference on Control and Automation, Christchurch, 2009, pp. 1318-1323.

[27] W. Ma, H. Qu, J. Zhao, B. Chen and G. Gui, "Sparsity aware normalized least mean p-power algorithms with correntropy induced metric penalty," 2015 IEEE International Conference on Digital Signal Processing (DSP), Singapore, 2015, pp. 638-642.

[28] Badong Chen, Lei Xing, Zongze Wu, Junli Liang, José C. Príncipe, Nanning Zheng, "Smoothed least mean p-power error criterion for adaptive filtering," Digital Signal Processing, vol. 40, pp. 154-163, 2015.

[29] W. Gao, J. Chen and L. Zhang, "Diffusion Approximated Kernel Least Mean P-Power Algorithm," 2019 IEEE International Conference on Signal Processing, Communications and Computing (ICSPCC), Dalian, China, 2019, pp. 1-6.

[30] X. Zhao, H. Xia, J. Zhao and F. Zhou, "Adaptive Wavelet Threshold Denoising for Bathymetric Laser Full-Waveforms With Weak Bottom Returns," in IEEE Geoscience and Remote Sensing Letters, vol. 19, pp. 1-5, 2022.

[31] H. Li, J. Shi, L. Li, X. Tuo, K. Qu and W. Rong, "Novel Wavelet Threshold Denoising Method to Highlight the First-break of Noisy Microseismic Recordings," in IEEE Transactions on Geoscience and Remote Sensing, doi: 10.1109/TGRS.2022.3142089.

[32] Da Zhang, Hongbo Zhao, Jiankun Yang, "Signal denoising of double-beam and double-scattering laser doppler velocimetry based on wavelet layering," Optik, Vol. 202, pp. 163545, 2020.

[33] Han, Hong-Gui, Qi-li Chen, and Jun-Fei Qiao. "An efficient self-organizing RBF neural network for water quality prediction," Neural Networks., vol. 24(7), pp. 717-725, 2011.

[34] Zhao, Tianxia, Xin'an Wang, and Changpei Qiu. "An Early Warning of Atrial Fibrillation Based on Short-Time ECG Signals." Journal of Healthcare Engineering 2022 (2022).

[35] Siddagangaiah, Roopa, and S. V. Narasimhan. "Improved evolutionary spectrum estimation using short time analytic discrete cosine transform with modified group delay." Mechanical Systems and Signal Processing 167 (2022): 108529.